PROCEEDINGS OF SPIE

SPIEDigitalLibrary.org/conference-proceedings-of-spie

A unique infrared spectropolarimetric unit for CRIRES+

Piskunov, Nikolai, Stempels, Eric, Lavail, Alexis, Escuti, Michael, Snik, Frans, et al.

Nikolai Piskunov, Eric Stempels, Alexis Lavail, Michael Escuti, Frans Snik, Andrey Dolgopolov, Milan Rozel, Candice Durandet, Artie Hatzes, Paul Bristow, Anna Brucalassi, Claudio Cumani, Reinhold J. Dorn, Andreas Haimerl, Ulrike Heiter, Renate Hinterschuster, Roman Follert, Derek Ives, Yves Jung, Florian Kerber, Barbara Klein, Jean-Louis Lizon, Thomas Marquart, Ignacio Molina-Conde, Luca Pasquini, Jérôme Paufique, Ernesto Oliva, Ansgar Reiners, Ulf Seemann, Jörg Stegmeier, Sebastien Tordo, Elena Valenti, "A unique infrared spectropolarimetric unit for CRIRES+," Proc. SPIE 10702, Ground-based and Airborne Instrumentation for Astronomy VII, 1070234 (6 July 2018); doi: 10.1117/12.2313512

SPIE.

Event: SPIE Astronomical Telescopes + Instrumentation, 2018, Austin, Texas, United States

A unique infrared spectropolarimetric unit for CRIRES+

Nikolai Piskunov[a], Eric Stempels[a], Alexis Lavail[a], Michael Escuti[b], Frans Snik[c], Andrey Dolgopolov[a], Milan Rozel[a], Candice Durandet[a], Artie Hatzes[d], Paul Bristow[e], Anna Brucalassi[e], Claudio Cumani[e], Reinhold J. Dorn[e], Andreas Haimerl[e], Ulrike Heiter[a], Renate Hinterschuster[e], Roman Follert[d], Derek Ives[e], Yves Jung[e], Florian Kerber[e], Barbara Klein[e], Jean Louis Lizon[e], Thomas Marquart[a], Ignacio Molina-Conde[e], Luca Pasquini[e], Jerome Paufique[e], Ernesto Oliva[f], Ansgar Reiners[g], Ulf Seemann[g], Jörg Stegmeier[e], Sebastian Tordo[e], and Elena Valenti[e]

[a]Department of Physics and Astronomy, Uppsala University, Box 516, SE-751 20 Uppsala, Sweden
[b]North Carolina State Univ, Dept Electrical & Computer Engineering, Raleigh, NC, USA
[c]Leiden Observatory, Leiden University, P.O. Box 9513, 2300 RA Leiden, The Netherlands
[d]Thüringer Landessternwarte, Sternwarte 5, D-07778 Tautenburg, Germany
[e]European Southern Observatory ESO, Karl-Schwarzschild-Strasse 2, D-85748 Garching bei München, Germany
[f]Arcetri Osservatori (INAF), largo E. Fermi 5, I-50125 Firenze, Italy
[g]Institut für Astrophysik, Georg-August Universität Göttingen, F. Hund Platz 1, D-37077 Göttingen, Germany

ABSTRACT

High-resolution infrared spectropolarimetry has many science applications in astrophysics. One of them is measuring weak magnetic fields using the Zeeman effect. Infrared domain is particularly advantageous as Zeeman splitting of spectral lines is proportional to the square of the wavelength while the intrinsic width of the line cores increases only linearly. Important science cases include detection and monitoring of global magnetic fields on solar-type stars, study of the magnetic field evolution from stellar formation to the final stages of the stellar life with massive stellar winds, and the dynamo mechanism operation across the boundary between fully- and partially-convective stars.

CRIRES+ (the CRIRES upgrade project) includes a novel spectropolarimetric unit (SPU) based on polarization gratings. The novel design allows to perform beam-splitting very early in the optical path, directly after the tertiary mirror of the telescope (the ESO Very Large Telescope, VLT), minimizing instrumental polarization. The new SPU performs polarization beam-splitting in the near-infrared while keeping the telescope beam mostly unchanged in the optical domain, making it compatible with the adaptive optics system of the CRIRES+ instrument.

The SPU consists of four beam-splitters optimized for measuring circular and linear polarization of spectral lines in YJ and HK bands. The SPU can perform beam switching allowing to correct for throughput in each beam and for variations in detector pixel sensitivity. Other new features of CRIRES+, such as substantially increased wavelength coverage, stability and advanced data reduction pipeline will further enhance the sensitivity of the polarimetric mode. The combination of the SPU, CRIRES+ and the VLT is a unique facility for making major progress in understanding stellar activity. In this article we present the design of the SPU, laboratory measurements of individual components and of the whole unit as well as the performance prediction for the operation at the VLT.

Keywords: Spectroscopy, Spectropolarimetry, Polarisation gratings, Stokes parameters

Ground-based and Airborne Instrumentation for Astronomy VII, edited by Christopher J. Evans, Luc Simard, Hideki Takami, Proc. of SPIE Vol. 10702, 1070234 · © 2018 SPIE · CCC code: 0277-786X/18/$18 · doi: 10.1117/12.2313512

1. INTRODUCTION

CRIRES[1] is a high spectral resolution ($R = 100000$) near-infrared spectrometer operated for several years at the ESO Very Large Telescope. While the instrument was rather unique due to its resolution, spectral range (1 to 5 μm) and integrated adaptive optics system, several parts, solutions and properties became unsatisfactory today. Examples are detectors, stability, calibration system and spectral coverage in a single exposure. The proposed upgrade that is nearing its completion will result in CRIRES+, an instrument that retains the best of the original system, while being retrofitted with new detectors, cross-dispersion, new calibration system, new metrology system and data reduction pipeline. These improvements in combination with cleaning, re-coating and re-aligning of the optical elements will result in higher throughput, up to a factor of 10 increase in simultaneous spectral coverage, much better stability and repeatability for standard settings. The data reduction will produce reliably calibrated science-quality spectra.

This paper describes the design and performance of the CRIRES+ spectropolarimetry unit (SPU). The design considerations presented below in Section 2 followed intensive optimization work looking for an acceptable compromise between CRIRES+ performance and minimum instrumental polarization. The preferred opto-mechanical solution consists of two pairs of beam-splitters for YJ and HK bands. In each pair one beam-splitter is preceded with a quarter-wavelength plate (QWP) for measurements of linear polarization. Section 3 describes the testing of the final product, both of the individual components by the manufacturer and of the final beam-splitter assemblies at Uppsala University. Finally, the opto-mechanical design of the SPU is shown in Section 4 and we conclude in Section 5.

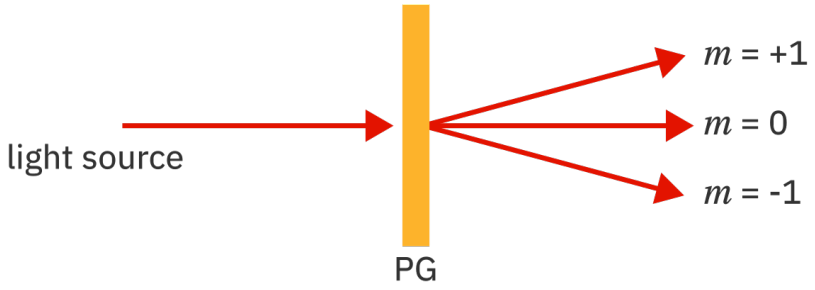

Figure 1. Schematic ray tracing for monochromatic light passing a PG. Part of the light continues undeviated to the $m = 0$ beam. The rest is separated between $m = +1$ and $m = -1$ according to circular polarization. The intensity ratio between $m = 0$ and the polarized beams changes dramatically at the threshold wavelength (0.95 μm in our case.)

2. SPU DESIGN

Description of the analysis, trade-off studies and final design was presented by Lockhart et al.[2] Here we give a quick summary of the arguments for the selected design. CRIRES+, as its predecessor CRIRES, uses a dedicated adaptive optics system (Multi-Application Curvature Adaptive Optics, MACAO) to increase the throughput at high-spectral resolution and stabilize the target image on the slit. This creates a problem for conventional polarimetric solutions. Splitting polarization into two beams after MACAO will introduce variable instrumental polarization that is very hard to correct. On the other hand, feeding two polarized beams to MACAO simultaneously will confuse the correction as the wavefront sensor will "see" two stars carrying inconsistent phase information. The adopted solution required a birefringent element that will separate polarizations in the science domain (wavelengths longer than 0.95 μm) but not for the MACAO wavefront sensor (wavelengths shorter than 0.95 μm). Such components are known as polarization gratings (PG, see e.g. Packham et al.[3]). A single PG separates the light in three orders (see Figure 1): $m = \pm 1$ contain left and right circularly polarized light while m=0 is unpolarized. The light goes to m=0 for wavelength shorter than the threshold while for longer wavelengths the polarized beams carry most of the light.

Combining two PGs creates an analogue of a modified Savart plate beam-splitter for circular polarization returning the polarized beams to the original propagation direction with a lateral shift depending on the distance

between two plates. PGs have a certain level of chromatism, i.e. the deviation angle for the $m = \pm 1$ beams increases with the wavelength. This effect forced us to develop separate beam-splitters for YJ (0.95 to 1.36 μm) and HK (1.48 to 2.54 μm) bands. CRIRES+ will not offer spectropolarimetry in L and M bands due to insufficient spacing between spectral orders. Measuring linear polarization is implemented by converting the incoming light to circularly polarized, which is commonly achieved by inserting a QWP in front of the beam-splitters.

Light losses due to PG chromatism can be minimized by accurately aligning the two polarized beams with the entrance slit of CRIRES+. In order to block the residual light in $m = 0$ beam at the science wavelength the slit is equipped with a two-hole decker. The holes extend by 2.5" on the sky in spatial direction separated by a 2.5" block.

Thus the critical parameters of the SPU are the optimization of the beam-splitters for the optical and the infrared bands, transition across the threshold wavelength, homogeneity and throughput. The implemented PGs were designed by Michael Escuti and his team using computer simulations. ImagineOptix (http://www.imagineoptix.com) manufactured samples from which we selected the best for the SPU beam-splitters. In the following section we present the characterization methodology and the final results.

3. CHARACTERIZATION OF THE POLARIZATION COMPONENTS

3.1 Polarization Gratings

A polarization grating is a birefringent film formed in this case by a liquid crystal polymer network, wherein the optic axis orientation is in-plane and varies linearly with position.[3] The PG simultaneously acts as a (circular) polarizing beam-splitter and spectral disperser of light. Physically PG consists of multiple thin film layers (3-5) with embedded periodic patterns.[4] The period defines the transition wavelength while subtle differences between layers are used to control transition slope and transmission ratio between polarized and unpolarized beams as function of wavelength. Particularly, the multiple chiral liquid crystal layers were fine-tuned to obtain a highly chromatic retardation.[5] This made it possible to fulfill the very stringent throughput specifications on the polarimeter, enabling an excellent zero-order transmission in the visible.

The naming convention for the beams refers to dispersion orders where $m_{\pm 1}$ are the first (polarized) orders and m_0 is the zero order. Thus the difference between the intensity in m_{+1} and m_{-1} gives the Stokes parameter V. The thin film is normally sandwiched between two glass substrates to protect the PG from environmental effects. Figure 2 shows one of the best six PGs optimized for the YJ bands. In practice, the manufacturing process allows making these device up to 150 mm in diameter with transition wavelengths anywhere between 0.4 and 2 μm.

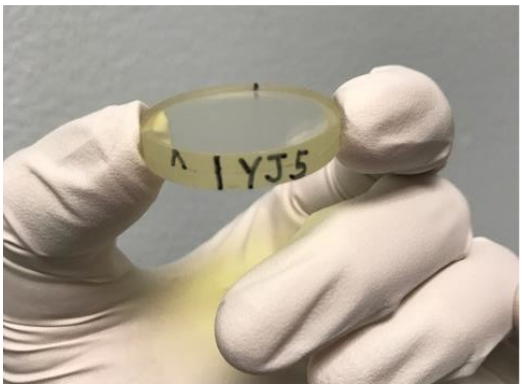

Figure 2. One of the SPU PGs optimized for YJ bands.

SPU PGs have a diameter of 27 mm and a thickness of 4.8 mm. Its flatness is $\lambda/10$ at 1000 nm and the enclosing plates are made of infrasil. Two types of PGs were developed for the CRIRES+ SPU: (a) HK PGs with a wavelength limits band from 1480 nm to 2540 nm, and (b) YJ PGs with a wavelength limits band from 960 nm to 1360 nm. This section describes tests performed by the manufacturer of the polarizing gratings

(ImagineOptix) at the premises of Geometric Phase Photonics Lab of the North Carolina State University. This characterization is to verify that the produced PGs and QWPs will deliver the required performance. The test results were used for selecting the two final sets of six PGs for each of the YJ and for HK bands (4 for two beam-splitters and 2 spares). The same technology was used by ImagineOptix to manufacture two QWPs for the HK band.[6] Analysis of these components is also presented below.

3.2 Characterization of PGs

All measurements in this section used as reference the detector readings with no PG in the beam. This is crucial for precision but limits the setup to measuring beams parallel to the optical axis. Figure 3 illustrates the setup for measuring the zeroth order transmission. The unpolarized collimated light from a monochromator is sent through a PG and a diaphragm to a single-pixel detector. Measurements were repeated for wavelengths from 400 nm to upper limit of PG range (1360 nm for YJ and 2540 nm for HK) with a typical resolution of 5 nm.

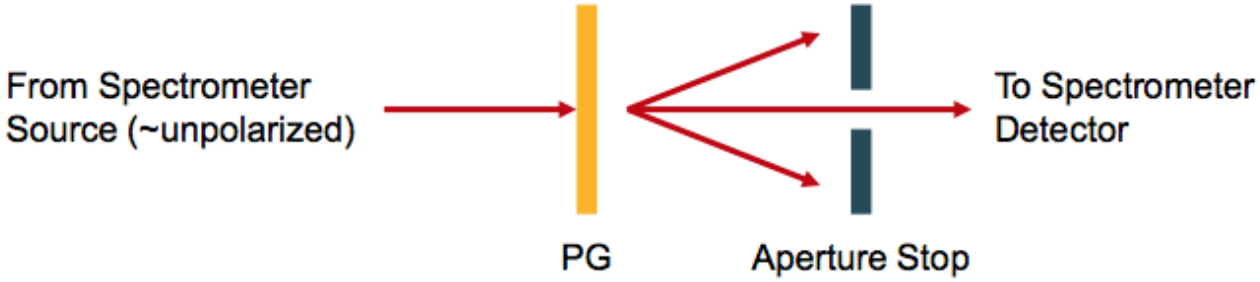

Figure 3. Schematic view of the setup for measuring throughput in $m = 0$ beam as function of wavelength.

In this test only the zero order ($m = 0$) relative intensity T_0 was measured directly. The amount of light going to the first orders ($m = \pm 1$) can be estimated as a complement of T_0 assuming no losses. Thus the transmittance of the first orders is $T_{+1} + T_{-1} \approx 1 - T_0$ (where T_{+1} and T_{-1} are the light intensity of the first orders).

Because a single PG transmittance of $T_{\pm 1}$ could not be measured directly the combined transmission in zero and first orders was measured for two PGs. An optical setup for this case is illustrated in Figure 4. The three beams that continue to the detector correspond to zeroth order of both PGs ($T_{0,0} = T_0^1 \times T_0^2$), m=-1, m=+1 ($T_{-1,+1} = T_{-1}^1 \times T_{+1}^2$, and m=+1, m=-1 ($T_{+1,-1} = T_{+1}^1 \times T_{-1}^2$). Here and below superscript refers to PG number and subscript refers to the polarization order. Unfortunately, there are other beams continuing at an angle to the optical axis, for example, m=0, m=±1 as shown in Figure 4.

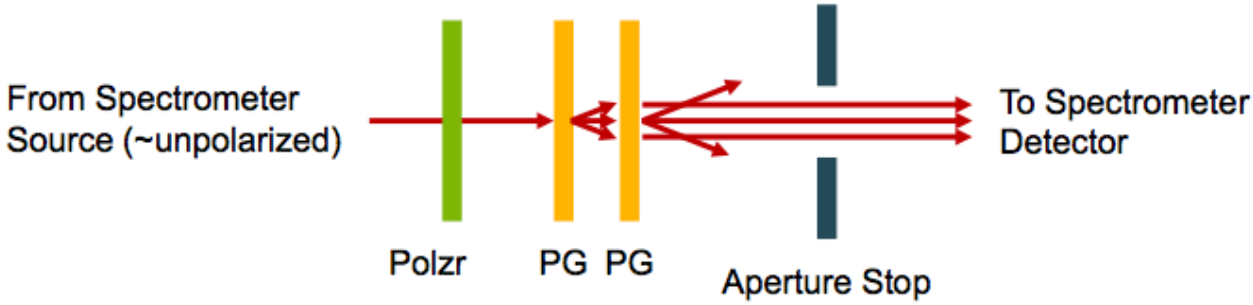

Figure 4. Double PG setup for measuring the sum of transmission for three beams. The two inclined arrows indicate the light directed into m=0 beam after the first PG and into m=±1 beams after the second. This light is lost for the measurements.

In this case the light is sent through a polarizer. Linearly polarized beam that can be represented as two beams of identical intensity circularly polarized in opposite directions. This guaranties identical intensities of the first order beams. Note that the PGs are combined in the same fashion as in the SPU beam-splitter.

The output zero and first order beams are selected using an aperture stop and measured together providing $T_0^1 \times T_0^2 + 2 \times T_1^1 \times T_1^2$. These measurements can be directly compared to the zero order measurements described in the beginning of this section assuming that $T_1^1 = (1 - T_0^1)/2$ and $T_1^2 = (1 - T_0^2)/2$.

The target requirements for the beam-splitters were set for the MACAO sensor domain (0.55 μm to 0.95 μm): minimum light to any beam that is not m=0, m=0; and for the science bands: maximum throughput for polarized m=$\pm$1, m=$\mp$1 beams.

3.3 HK PGs transmittance

Figure 5 shows measurements of m=0 throughput for the 6 best PGs optimized for the HK band. These measurements are obtained using the setup of Figure 3. The sum of $T_{+1} + T_{-1}$ was estimated as $1 - T_0$.

Optimization was easier in HK case because of the location of the science bands the transition did not have to be very steep and could be shifted to 1 μm.

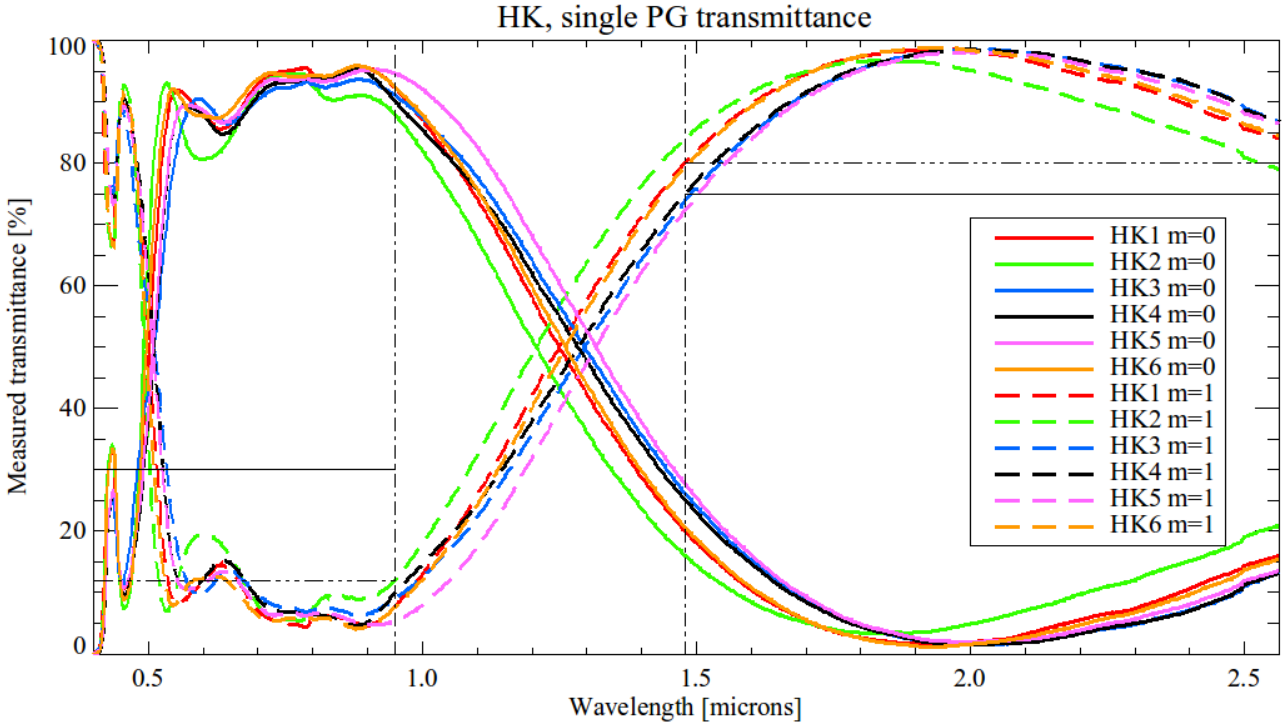

Figure 5. Measurements of $m = 0$ (solid lines) and $m = \pm 1$ (dashed lines) relative beam intensity for the 6 best PGs optimized for HK bands. Horizontal solid and dash-dotted lines shows the derived requirements (maximum and goal in the visible and minimum and goal in the infrared) for the sum of polarized beams. The dash-dotted vertical lines show the transition wavelength defined by the CRIRES+ dichroic window and the start of the H-band.

All six PGs fulfill our requirements. Small shifts of transmission curves in wavelength, as seen in Figure 5, represent an attempt by the manufacturer to find the optimal performance across the infrared bands. These shifts provide extra flexibility when selecting PG pairs for the beam-splitters.

The SPU includes one circular polarization beam-splitter for HK bands and one beam-splitter for HK bands combined with an achromatic quarter-wave retarder plate for linear polarization. The image separation on the entrance slit is defined by the separation of the two PGs, which is 18 mm in the case of the HK beam-splitter.

3.4 YJ PGs transmittance

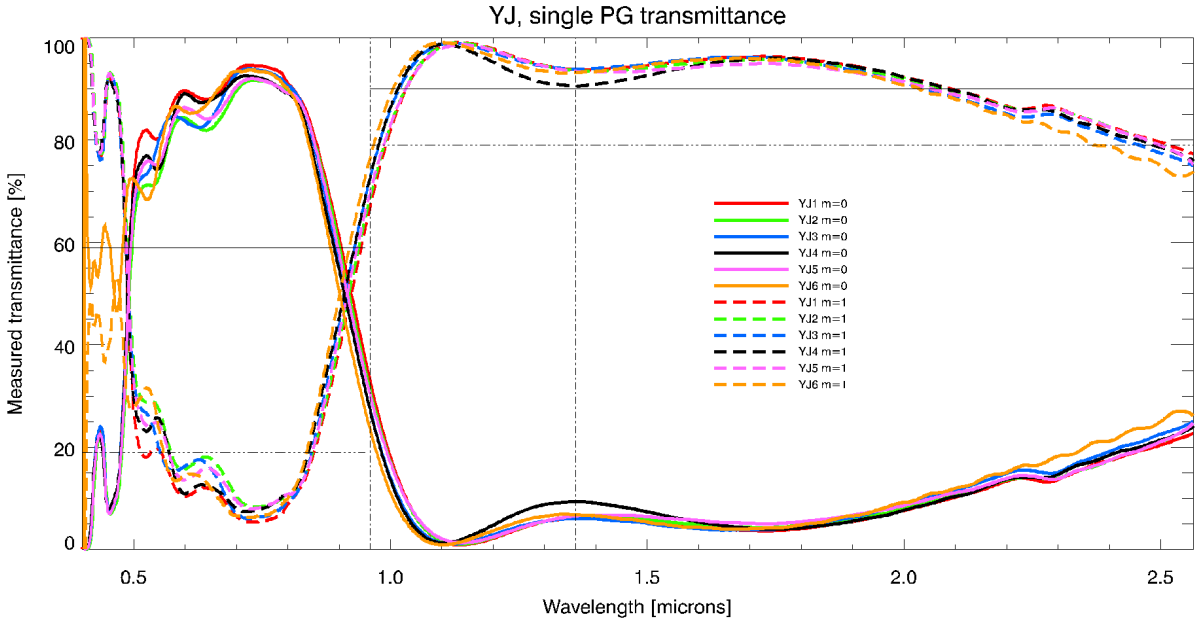

Figure 6. Measurements of $m = 0$ (solid lines) and $m = \pm 1$ (dashed lines) relative beam intensity for the 6 best PGs optimized for YJ bands. Horizontal solid and dash-dotted lines shows the derived requirements (maximum and goal in the visible and minimum and goal in the infrared) for the sum of polarized beams. The dash-dotted vertical lines show the start of the Y and J bands.

The optimization task for the short wavelength PGs was much more challenging because there is no space for gradual transition from optical to infrared regime. While it is possible to achieve a very steep transition slope, it results in large oscillations of transmission between m=0 and m=±1 beams on both sides of the transition wavelength. In the end a compromise was found that produces acceptable science throughput (at wavelengths larger than 0.95 μm) and does not compromise the performance of MACAO. Figure 6 shows the measured transmittance for the best YJ gratings that fulfill the science requirements. Compatibility with the MACAO system is maintained because of two reasons: (a) the sensitivity peak of MACAO detector coincides with the minimum of m=±1 beam transmittance around 0.7-0.8 μm, and (b) m=±1 beams are dispersed in wavelength as opposed to m=0 beam enhancing the contrast of the central image. Measurements with telescope simulator, turbulence generator, SPU and MACAO confirmed stable closed-loop operation of the of the AO.

3.4.1 Beam-splitter verification tests

All four beam-splitters were assembled and aligned at the Department of Physics and Astronomy of Uppsala University. The test setup included a light source (30 W incandescent element producing a 1200 K blackbody flux), a monochromator (LOT MSH-300F), a point source simulator and two cameras: a CCD camera ZWO ASI178MM for the optical domain and a CEDIP TITANIUM for the infrared. The IR camera sensitivity range was between 1.2 and 5 μm. The setup was used for several purposes, most importantly for verifying the PG separation and alignment, and controlling the transmittance of the assemblies. The alignment is a non-trivial task. When misaligned, a pair of PGs produces seven images of the point source, all with different directions of light propagation. Their separations from the central image depend both on the misalignment and the wavelength. Therefore, for aligning a beam-splitter, one of the two PGs was fixed at the base of the mechanical mount while the other was rotated with a fixed step by a rotation stage. Images taken at each angular position were analyzed and the optimal position was usually determined with an accuracy better than 30 arcminutes. This accuracy translates to the alignment of the three images on the entrance slit of CRIRES+ that is approximately 2 % of the slit width. The alignment was performed using optical light and verified with the infrared imaging where

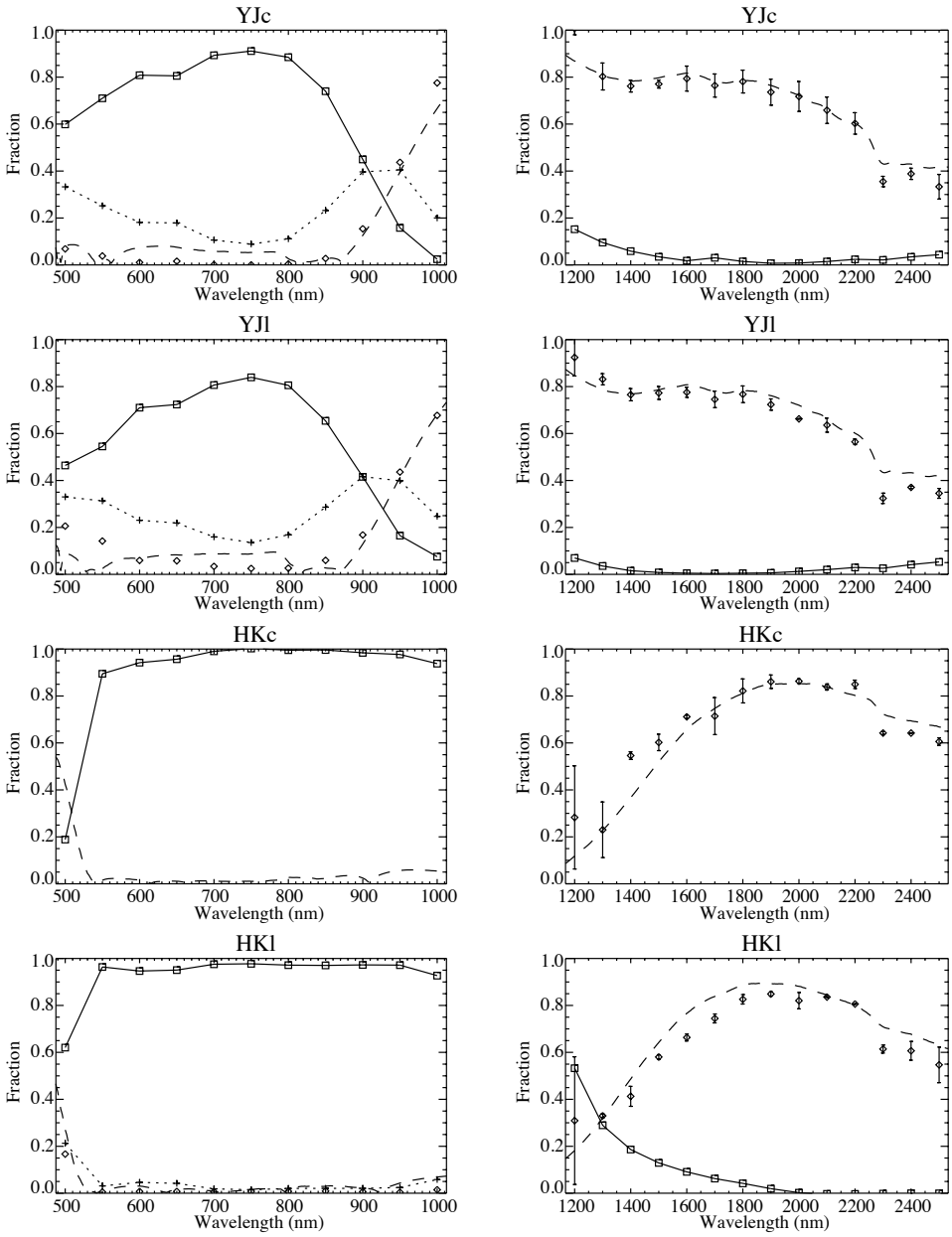

Figure 7. Transmittance measurements of the SPU beam-splitters. Each row of panels correspond to one beam-splitter. Squares are $T_{0,0}$ transmittance while diamonds are the sum of the science beams $T_{+1,-1} + T_{-1,+1}$. Dashed and dotted lines are estimated performance of the beam-splitters based on single-PG measurements by the manufacturer.

the spot separation is larger (due to PG dispersion), but the camera pupil was insufficient to register the light in all beams simultaneously.

The transmittance measurements without beam-splitters were used for normalization. Figure 7 shows the beam-splitter transmittance measurements compared to transmission curved for individual PG shown in Figures 5 and 6. The agreement is fairly good showing that the behavior of individual components and the whole assembly is well understood. The dotted line shows the intensity of the m=0,±1 ghosts whenever these could be measured. These ghosts were the main concern for the stable operation of the AO but its spectral distribution resulted in minimum disturbance for the wavefront sensor.

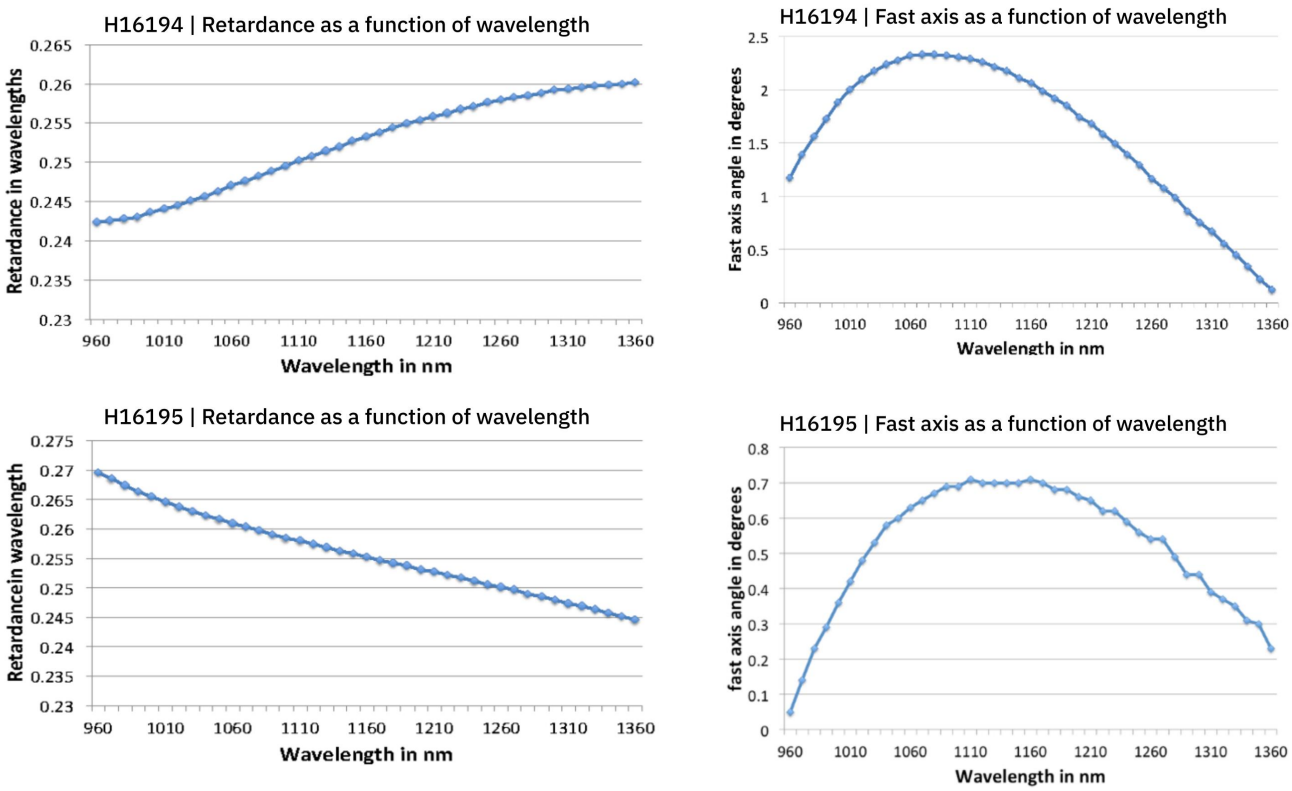

Figure 8. Measured YJ QWP performance as function of wavelength. The two rows describe two retarders. Left panel shows retardance in wavelength fraction while fast axis orientation in degrees is shown on the right.

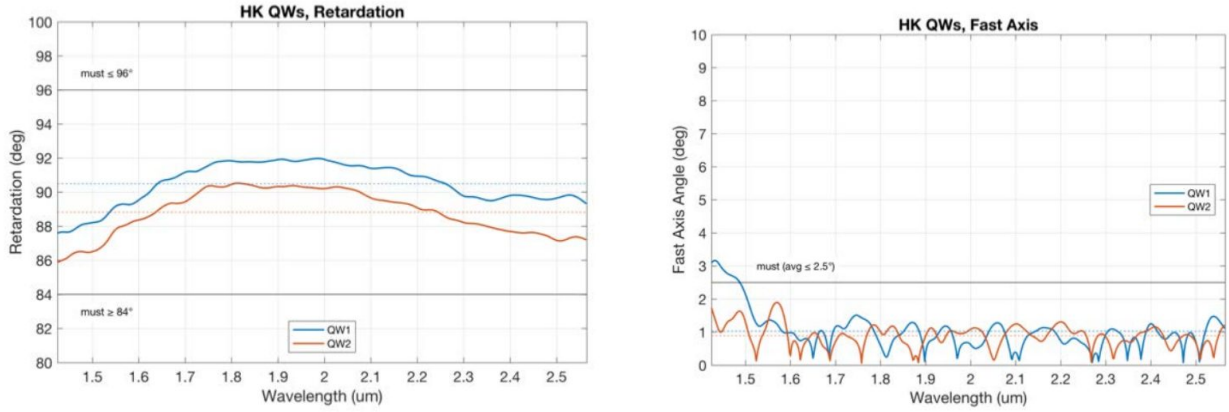

Figure 9. Measured HK QWP performance as function of wavelength. Left panel shows retardance in degrees. The two horizontal lines indicate the requirements. Fast axis orientation variation is shown on the right.

3.5 Quarter wavelength plates

The SPU uses QWPs in combination with beam-splitters for measuring linear polarization. The QWP technology differs for YJ and HK bands. The YJ super-achromatic retarders are based on multi-layer stretch polymers designed and manufactured by Meadowlark. The HK QWPs are using polymerized liquid crystals, a technology similar to the manufacturing of PGs. These were produced by ImagineOptix. Performance measurements consisted of characterizing the variation with wavelength of the retardance, fast axis orientation, transmission

and uniformity. Requirements on these criteria are based on the science case for detecting rotational modulation of magnetic fields in M-dwarfs and newly formed solar-type stars.

Retardance and fast axis orientation were measured by inserting two polarizers on both sides of a QWP. The first polarizer was oriented at 45 degrees relative to the fast axis of the QWP. The second (exit) polarizer was rotated to measure the polarization ellipse at various wavelengths. Deviations from perfect circle were interpreted in terms of retardance and fast axis rotation. The four plates including the spares have shown excellent performance matching or even exceeding the requirements. Fig. 8 shows the measurements results for the YJ plates. The retardance gradually changes from 87.3° to 93.6° for H16194 plate and from 97.2° to 88.2° for H16195, which should be compare to the set requirement of ±6°. The fast axis orientations are constant to within ±1.12° and ±0.35° to be compared to a requirement of ±1.25°. Thus H16194 was a clear first choice.

For the HK bands both retarder plates are well within the requirements for the retardance (Fig. 9). QW2 was selected due to more homogeneous variations of the fast axis.

In addition to these parameters the throughput and homogeneity were studied. The throughput (transmittance) of the YJ QWPs was higher than 90 %. The same parameter for the HK QWP was found to be over 93 %.

4. OPTO-MECHANICAL DESIGN

Spectro-polarimetric measurements impose stringent requirements on the mechanical components and moving functions of the SPU. For each particular Stokes parameter and particular wavelength setting the SPU must insert the correct beam-splitter into the telescope beam. In order to account for difference in the throughput along the two optical paths of the $m = \pm 1$ beams the SPU also should provide a possibility for switching the beams. For example, for measuring Stokes Q in H-band the SPU should insert an HK QWP and an HK beam-splitter, orient the QWP according to the coordinate system on the sky and align the beam-splitter with the slit. During the exposure the QWP should rotate to compensate for the rotation of the field-of-view in the Nasmyth focus of the VLT. Note that the SPU is located before the image derotator which means this cannot be used in this mode.

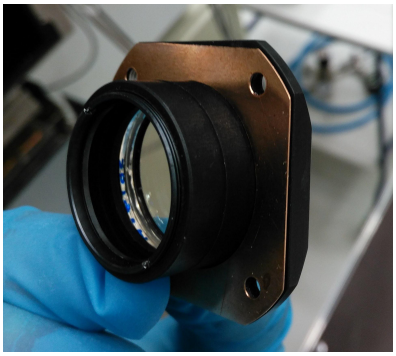

Figure 10. Science beam-splitter for HK band.

In the same time, the beam-splitters themselves should provide a highly repeatable and stable separation independent of orientation. Thus the beam-splitters consist of two cylinders each holding a PG. The two cylinders are attached to each other with a fine thread that allows precise alignment of the PGs while keeping the separation within tolerances (for an f/15 telescope beam the tolerance on PG separation was ±0.5mm). After the alignment the position was fixed with thread locker. Figure 10 shows a photo of a fully assembled beam-splitter for HK bands.

The proper orientation of the beam-splitters and QWPs is preserved by mounting these components on the side of the SPU turret (Fig. 11). The turret has two (non-identical) sides with openings. Four fairly flat rotation stages SR-7012 from SmarAct (http://www.smaract.com/products/rotary-positioners) mounted on the turret walls carry two beam-splitters (one for YJ and one for HK) and two QWPs. In the CAD image

Figure 11. Mechanical design of the SPU. The turret carries beam-splitters and QWPs, some mounted on rotation stages. The whole turret can rotate around vertical axis.

we see from left to right a YJ linear polarization, an HK circular, an HK linear and YJ circular beam-splitters. Only circular beam-splitters are mounted on rotation stages. Linear beam-splitters are manually aligned with the entrance slit of CRIRES+ and fixed in that position. The opposite side of the turret carries two QWPs on similar rotation stages.

In order to align the optical axis of the beam-splitters (and QWPs) with the telescope optical axis the

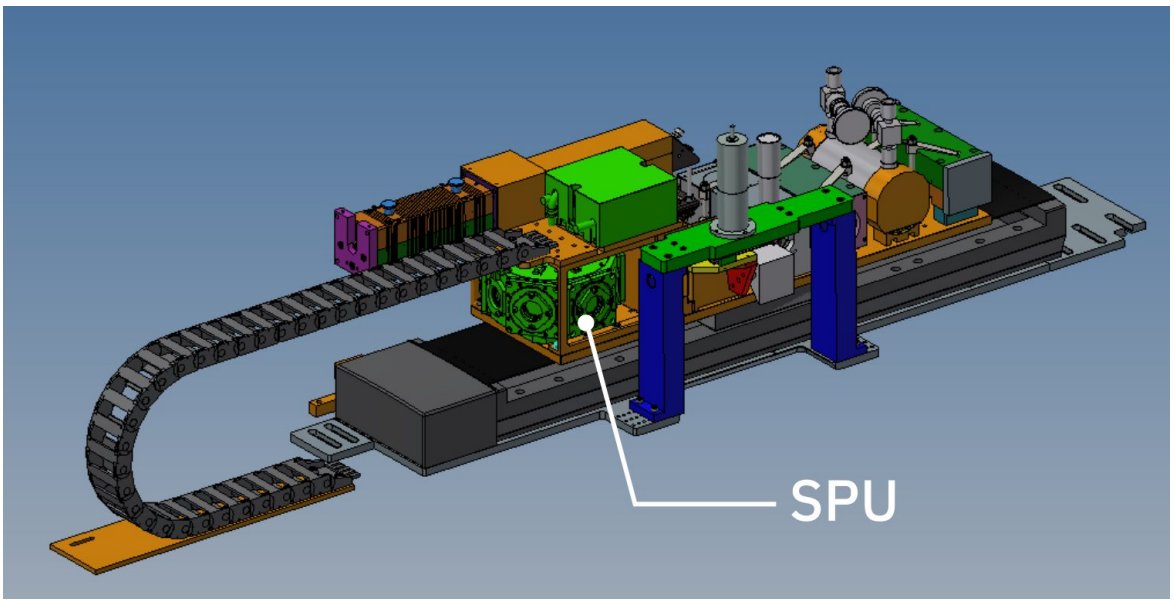

Figure 12. Calibration slider of CRIRES+.

turret is mounted on a U-660 rotation stage from PI (https://www.physikinstrumente.com/en/products/rotation-stages/) and thus can rotate around a vertical axis. The choice to use piezo motors resulted in a very compact design while achieving high-speed and no central obscuration. The SR-7012 motors make a 180° turn for beam switching in less than 4 seconds – comparable with detector readout. Built-in encoders ensure a positioning precision of a few arcseconds. The PI motor makes full rotation in less than a second. The PI motor has no restriction on the number of rotations but this could result in winding of the SR-7012 motor cables. To prevent this we have a two-stage limit sensor system: a Hall sensor and a soft "hard" stop. The design of the turret also balances the weight minimizing the torque on the PI motor. The expected longevity of the moving functions is expected to be at least five years assuming nightly use.

The whole SPU is located on a calibration slider which is shared with many other subsystems (Fig. 12). A translation motion of the slider brings one component at a time to the optical axis of the telescope. Figure 12 shows the slider from the telescope side. The SPU is the left-most instrument on the slider. The roof of the SPU carries the sensor units for the SR-7012 motors and cable connectors but also the hollow-cathode lamp assembly. The limit switches are mounted at the bottom of the roof. Complex densely-packed equipment and moving functions required a cable wrap to be attached to the slider.

5. CONCLUSIONS

- The SPU was manufactured and optical and polarimetric performances are found to be matching the requirements.
- Mechanical functionality was successfully tested for speed and reliability.
- At least in the tests with turbulence generator and telescope simulator MACAO operation is stable with SPU HK and YJ beam-splitters without any additional corrective actions such as restricting the wavelengths of the light going to the wavefront sensor.
- In HK bands MACAO+SPU delivers essentially the same performance as without SPU.
- In YJ bands the performance is slightly worse, possibly due to reduced transmittance. This test will need to be repeated using the CRIRES+ slit viewing camera with the appropriate filters. However, we do not expect the conclusion about stability of MACAO operation to change.
- Additional tests of moving functions operation by the instrument control system will be required before installation at the telescope.

Considering the positive results from the SPU test measurements we expect to be able to achieve better than 10^{-3} sensitivity for circular polarization (Stokes parameter V) for solar-type and cooler stars. We expect the performance to be slightly better for HK bands, which is of particular interest. It also opens an opportunity to study magnetic sensitivity of resonance lines for some heavy elements in hot stars as was predicted by theoretical atomic structure calculations. Linear polarization (Stokes parameters Q and U) should reach 10^{-3} sensitivity. It was demonstrated that the a reliable reconstruction of magnetic fields on rapidly rotating stars requires time series of all four Stokes parameters.[7,8] Thus, the ability to measure Q and U in addition to V is crucial for successful application of the Magnetic Doppler Imaging to cool stars. For now, CRIRES+ – and SPIRou[9] – will be the only instruments at a large telescope to access the high-resolution near-infrared full Stokes vector, which will allow to tremendously improve our knowledge of cool objects in the universe.

ACKNOWLEDGMENTS

The authors are thankful to the Knut and Alice Wallenberg Foundation in Sweden for generous support of the CRIRES+ project and the development of the SPU unit in particular.

REFERENCES

[1] Käufl, H. U., Ballestera, P., Biereichela, P., Delabre, B., Donaldson, R., Dorn, R., Fedrigo, E., Finger, G., Fischer, G., Franza, F., Gojak, D., Huster, G., Jung, Y., Lizon, J.-L., Mehrgan, L., Meyer, M., Moorwood, A., Pirard, J.-F., Paufique, J., Pozna, E., Siebenmorgen, R., Silber, A., Stegmeier, J., and Wegerer, S., "Crires: A high resolution infrared spectrograph for esos vlt," *Proc. SPIE* **5492**, 1218–1227 (2004).

[2] Lockhart, M., Piskunov, N., Stempels, E., Escuti, M., Oliva, E., Käufl, H.-U., Heiter, U., Marquart, T., Anglada-Escude, G., Baade, D., Bristow, P., Dorn, R., Follert, R., Gojak, D., Grunhut, J., Hatzes, A., Hilker, M., Ives, D., Jung, Y., Kerber, F., Klein, B., Lizon, J.-L., Löwinger, T., Origlia, L., Pasquini, L., Paufique, J., Pozna, E., Reiners, A., Seemann, U., Smette, A., Smoker, J., and Valenti, E., "Novel infrared polarimeter for the eso crires+ instrument," *Proc. SPIE* **9147**, 8–14 (2014).

[3] Packham, C., Escuti, M., Ginn, J., Oh, C., Quijano, I., and Boreman, G., "Polarization Gratings: A Novel Polarimetric Component for Astronomical Instruments," *Publications of the Astronomical Society of the Pacific* **122**, 1471 (Dec. 2010).

[4] Oh, C. and Escuti, M. J., "Achromatic diffraction from polarization gratings with high efficiency," *Optics Letters* **33**, 2287 (Oct. 2008).

[5] Hornburg, K. J., Komanduri, R. K., and Escuti, M. J., "Multiband retardation control using multi-twist retarders," in [*Polarization: Measurement, Analysis, and Remote Sensing XI*], **9099**, 90990Z (May 2014).

[6] Komanduri, R. K., Lawler, K. F., and Escuti, M. J., "Multi-twist retarders: broadband retardation control using self-aligning reactive liquid crystal layers," *Optics Express* **21**, 404 (Jan. 2013).

[7] Kochukhov, O. and Piskuniv, N., "Doppler imaging of stellar magnetic fields. ii. numerical experiments," *Astronomy & Astrophysics* **388**, 868–888 (2002).

[8] Rosén, L., Kochukhov, O., and Wade, G. A., "First Zeeman Doppler Imaging of a Cool Star Using all Four Stokes Parameters," *ApJ* **805**, 169 (June 2015).

[9] Parès, L., Donati, J.-F., Dupieux, M., Gharsa, T., Micheau, Y., Bouye, M., Dubois, B., Gallou, G., Kouach, D., Barrick, G., and Wang, S.-Y., "Front end of the SPIRou spectropolarimeter for Canada-France Hawaii Telescope," in [*Ground-based and Airborne Instrumentation for Astronomy IV*], *Proc. SPIE* **8446**, 84462E (Sept. 2012).